Multiwavelength Astrophysics Laboratory

Module III: High-Energy Astrophysics

THE SKY SEEN IN GAMMA-RAYS

Ettore Bronzini
University of Bologna & INAF-OAS

Slides based on Prof. P. Grandi lessons at the University of Bologna


High-Energies (HE)
~30 MeV - 100 GeV
Very high-Energies (VHE)
~100 GeV - 100 TeV
MAGIC
VERITAS
LHAASO
HESS
CTAO-N
CTAO-S
Fermi
AGILE

WHAT WE OBSERVE

Observed emission in gamma-ray band **cannot** be explained in terms of thermal radiation

—> **NON-THERMAL PROCESSES**

LEPTONIC

Given a PL distribution of electron energies

$$\mathcal{N}\left(\gamma_e\right) = K\gamma_e^{-p}, \quad \gamma_{\min} < \gamma_e < \gamma_{\max}$$

Sync. energy density

$$\epsilon_{\mathrm{s}}(\nu) \propto K\, B^{(p+1)/2} \nu^{-(p-1)/2}$$

IC energy density

$$\epsilon_{\mathrm{c}}(\nu) \propto K \nu^{-\alpha} \int \frac{U_r(\nu)\nu^{\alpha}}{\nu} d\nu$$

B magnetic field

$U_r(\nu)$ seed photon density

$$\alpha = \frac{p-1}{2}$$

HADRONIC

$$p + p \rightarrow \pi^{\pm}, \pi^0, K^{\pm}, K^0, p, n\ldots$$

$$p + \gamma_\epsilon \rightarrow \Delta^+ \rightarrow \pi^0 + p$$
$$\rightarrow \pi^+ + n$$

where $\pi^0 \rightarrow 2\gamma$

DETECTORS

Pair conversion telescope

$$\gamma \rightarrow e^- + e^+$$

Incoming gamma rays pass freely through the thin plastic **anticoincidence** detector, while charged cosmic rays cause a flash of light. A gamma ray continues until it interacts with an atom in one of the **conversion foils**, producing two charged particles: an electron and a positron. They proceed on, creating ions in thin silicon strip detectors. Finally the particles are stopped by a **calorimeter** which measures the total energy deposited.

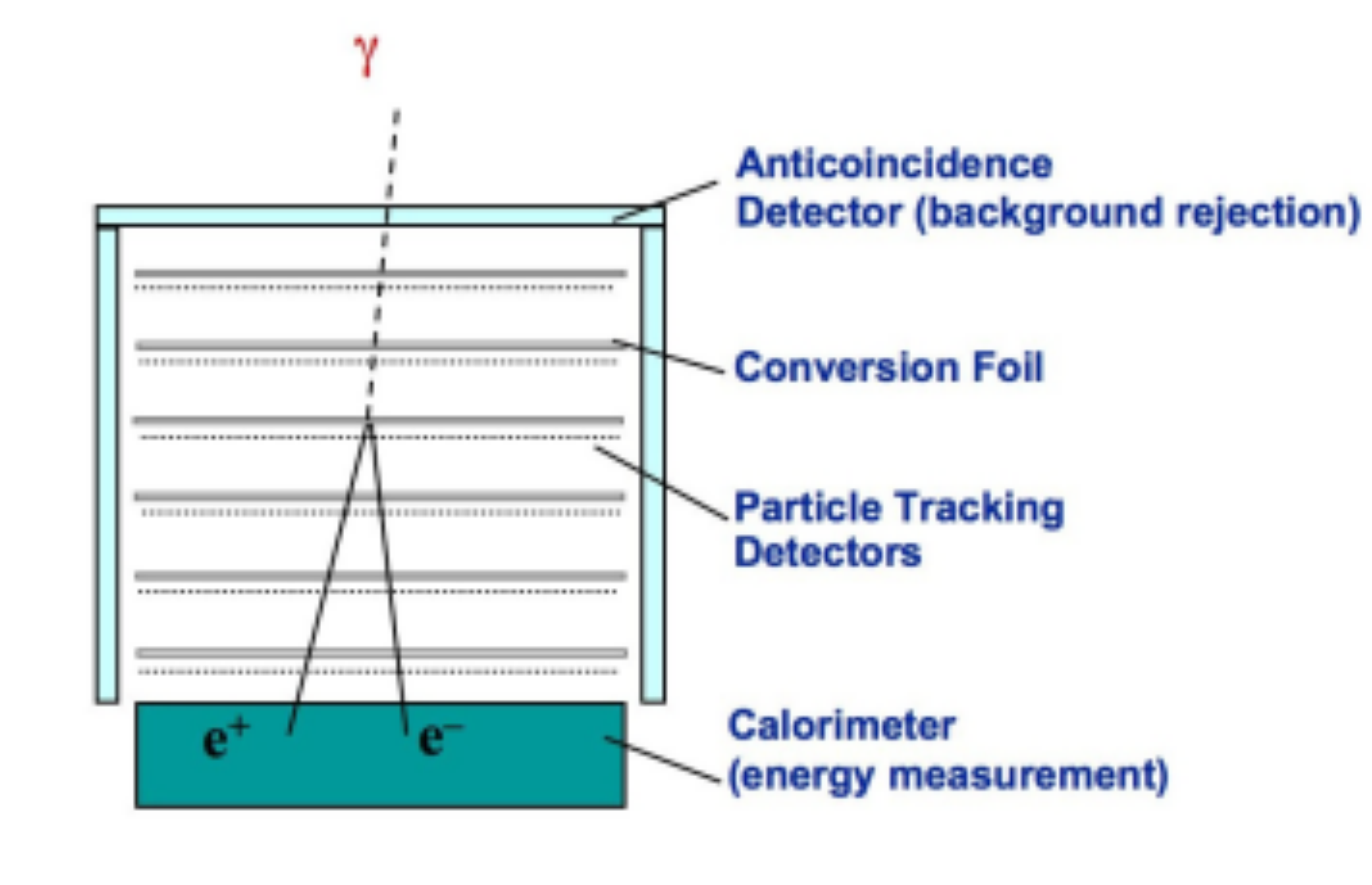

DETECTORS

Pair conversion telescope

$$\gamma \rightarrow e^- + e^+$$

Incoming gamma rays pass freely through the thin plastic **anticoincidence** detector, while charged cosmic rays cause a flash of light. A gamma ray continues until it interacts with an atom in one of the **conversion foils**, producing two charged particles: an electron and a positron. They proceed on, creating ions in thin silicon strip detectors. Finally the particles are stopped by a **calorimeter** which measures the total energy deposited.

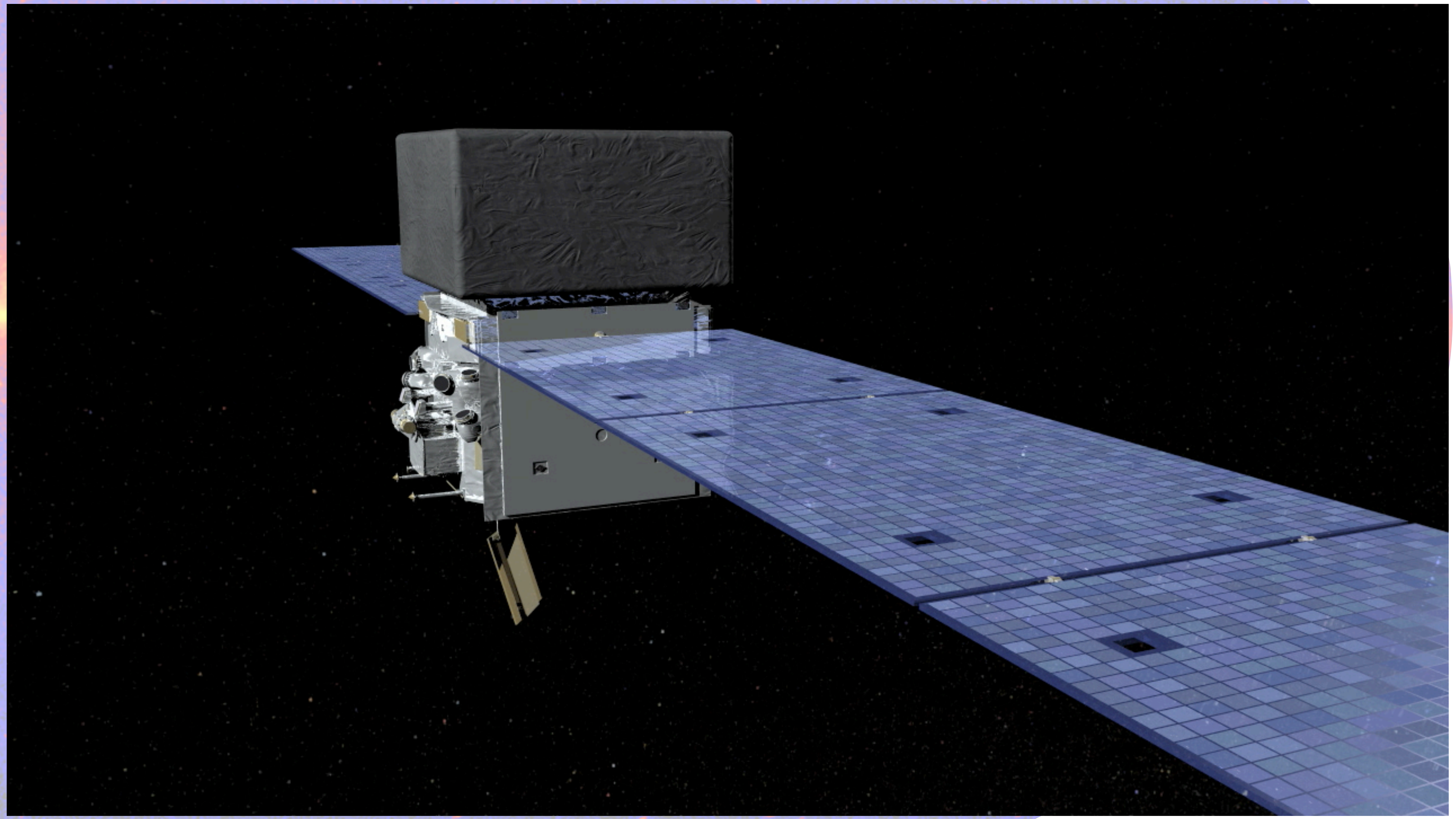

FERMI SATELLITE

Operation mode: **survey mode with a full-sky coverage every 2 orbits (3hrs)**

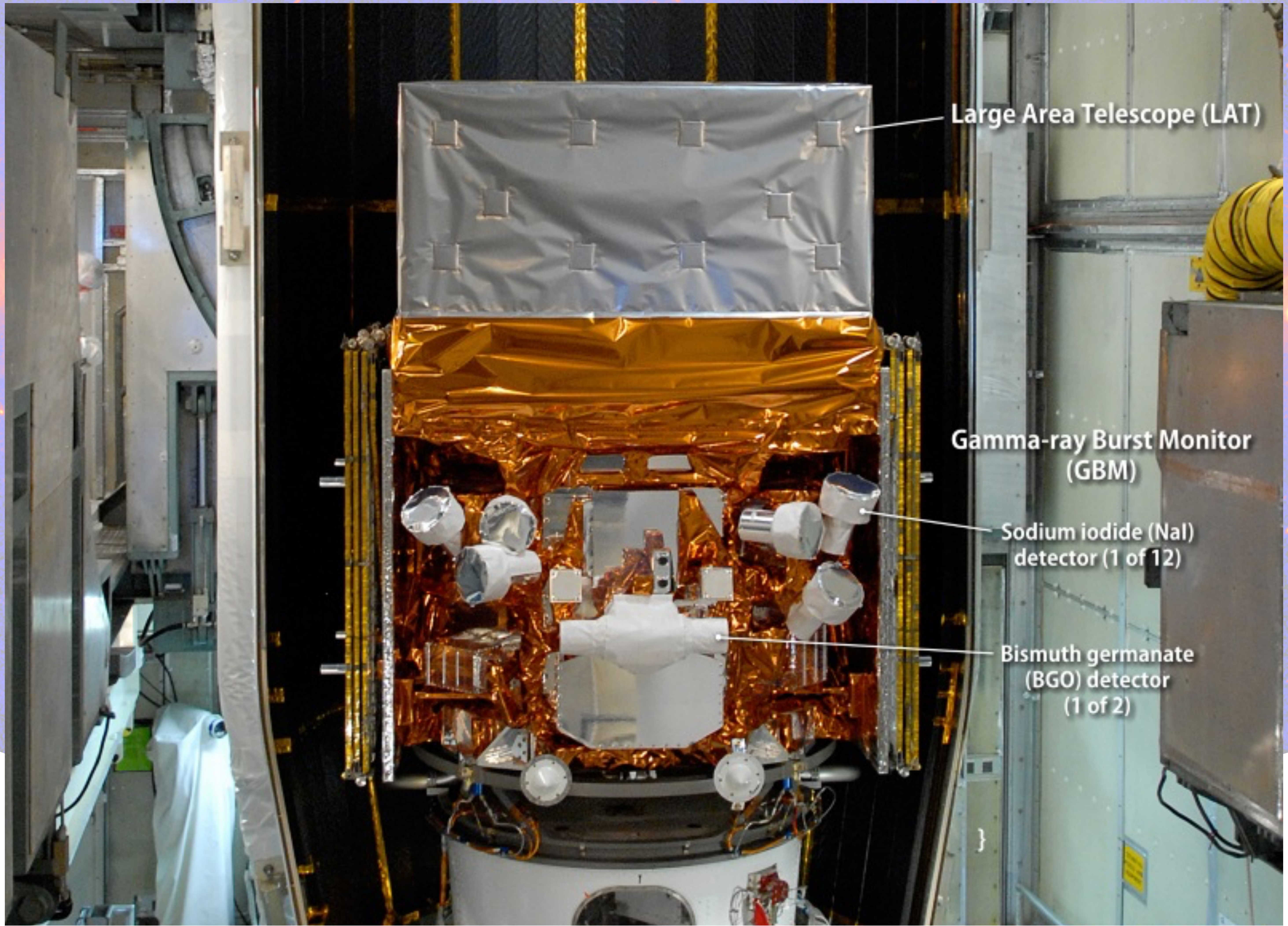

LARGE AREA TELESCOPE

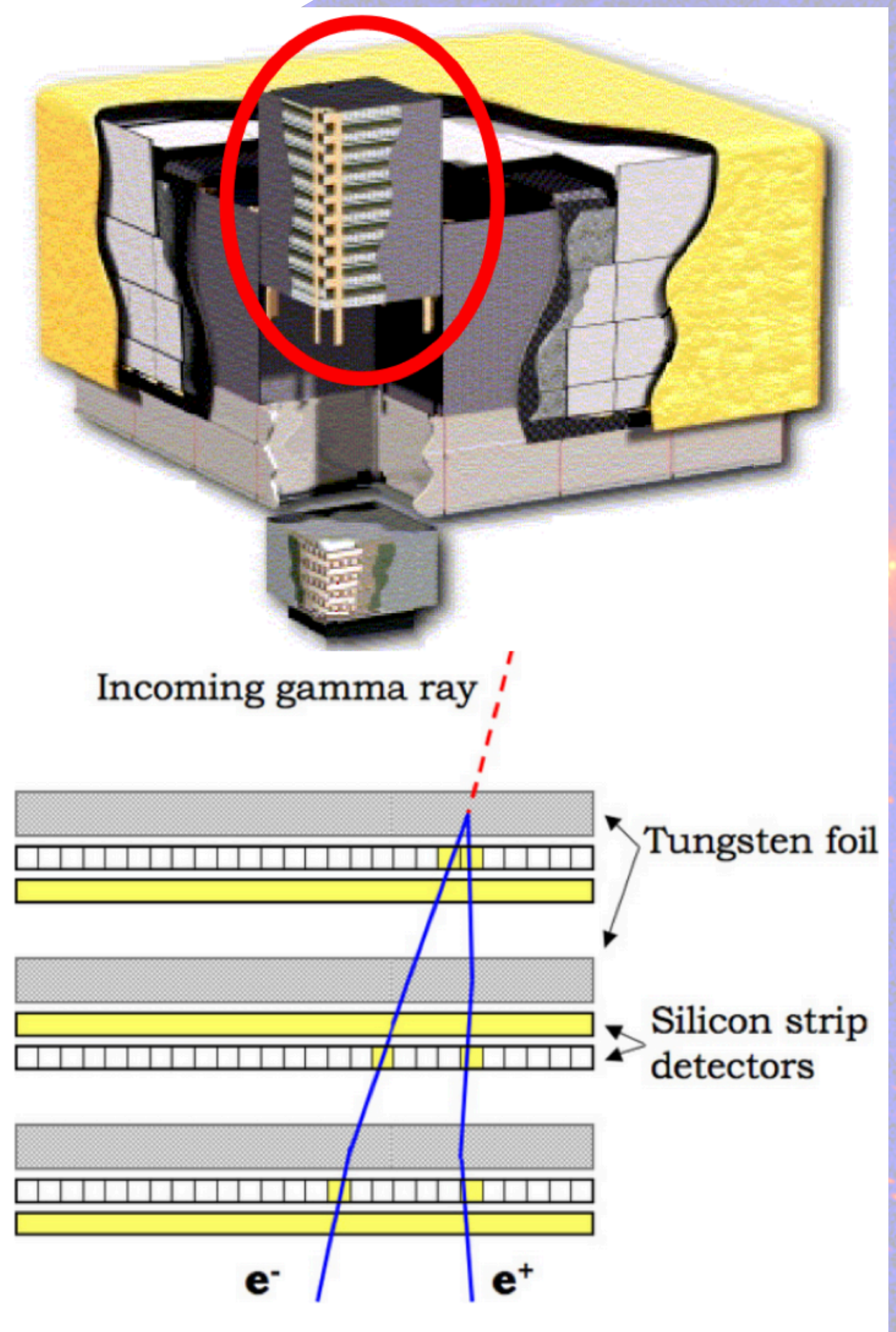

Picture of a tracker plane:

The LAT detects γ-rays in the energy range from **20 MeV to ~2 TeV**, measuring their arrival times, energies, and directions.

- 16 modular towers
  - 18 tungsten converter layers
  - 16 dual silicon tracker planes
    - 12 thin layers on the top (***front* section**)
    - 4 thick layers on the bottom (***back* section**)

Each of the 16 calorimeter modules consists of 96 long, narrow CsI scintillators, stacked in 8 layers, alternating in orientation so that the location and spread of the deposited energy can be determined.

LAT DATA FORMAT

- **photon files** (aka scientific files):
  for each event, includes the energy, the sky arrival direction, the quality of the reconstructed event. It also includes GTI.

Select	ENERGY	RA	DEC	L	B	THETA	PHI	ZENITH_ANGLE	EARTH_AZIMUTH_ANGLE	TIME	EVENT_ID
	E	E	E	E	E	E	E	E	E	D	J
All	MeV	deg	deg	deg	deg	deg	deg	deg	deg	s	
Invert	Modify	Modify	Modify	Modify	Modify	Modify	Modify	Modify	Modify	Modify	Modify
1	1.024935E+02	1.890637E+02	4.887585E+01	1.296221E+02	6.805478E+01	3.311039E+01	1.545781E+02	6.648592E+01	3.855091E+01	2.395579495640E+08	1499902
2	8.548724E+03	1.844947E+02	4.871450E+01	1.374336E+02	6.746097E+01	7.881751E+01	3.575599E+02	1.121413E+02	3.180587E+02	2.395605824415E+08	3365803
3	4.587276E+02	1.882033E+02	4.872671E+01	1.311867E+02	6.810202E+01	7.670603E+01	3.590155E+02	1.099964E+02	3.179321E+02	2.395605964979E+08	3394549
4	1.787166E+02	1.800865E+02	4.572431E+01	1.482148E+02	6.881462E+01	2.222104E+01	2.357567E+02	5.720790E+01	2.317117E+01	2.395698295218E+08	8718051
5	8.558330E+01	1.837057E+02	4.752892E+01	1.398792E+02	6.837653E+01	7.378289E+01	3.461026E+02	1.055196E+02	3.156298E+02	2.395717697642E+08	400736
6	1.835469E+03	1.869453E+02	4.893111E+01	1.332178E+02	6.772206E+01	4.873021E+01	7.576329E+01	7.949971E+01	4.156288E+01	2.395802562035E+08	4873353
7	1.422232E+02	1.805116E+02	4.749071E+01	1.450752E+02	6.745815E+01	4.611554E+01	7.095655E+01	7.604772E+01	4.412677E+01	2.396032045441E+08	3810555
8	8.920106E+01	1.864955E+02	4.862397E+01	1.341833E+02	6.794450E+01	3.354660E+01	1.491865E+02	6.700893E+01	3.844512E+01	2.396152818320E+08	6007701
9	1.672174E+02	1.869159E+02	4.830136E+01	1.336816E+02	6.832774E+01	7.213040E+01	3.488381E+02	1.046863E+02	3.168086E+02	2.396177444197E+08	12708295
10	4.423530E+02	1.855420E+02	4.861044E+01	1.357987E+02	6.778015E+01	7.637954E+01	3.572539E+02	1.098098E+02	3.181917E+02	2.396179385276E+08	13076259
11	1.376245E+02	1.822363E+02	4.813775E+01	1.416184E+02	6.741972E+01	6.654009E+01	5.058924E+01	9.752274E+01	2.643031E+01	2.396254579644E+08	4391977
12	2.094003E+02	1.872630E+02	4.830079E+01	1.330747E+02	6.838431E+01	3.717078E+01	2.957832E+02	6.998155E+01	3.571473E+02	2.396278463736E+08	10130810
13	6.923818E+02	1.849774E+02	4.784232E+01	1.374045E+02	6.839037E+01	7.719269E+01	3.595765E+02	1.106789E+02	3.179611E+02	2.396294471081E+08	15577911
14	4.603773E+02	1.844559E+02	4.782698E+01	1.383101E+02	6.828523E+01	7.885845E+01	4.217021E+01	1.128288E+02	3.577484E+02	2.396420389208E+08	6878194
15	3.958750E+02	1.854190E+02	4.865240E+01	1.359700E+02	6.771561E+01	7.824626E+01	7.339544E+00	1.124857E+02	3.217743E+02	2.396468240380E+08	3561844
16	1.522196E+02	1.807202E+02	4.786566E+01	1.442811E+02	6.720000E+01	7.612041E+01	3.505654E+02	1.090533E+02	3.166456E+02	2.396579508791E+08	810339
17	6.740921E+02	1.835186E+02	4.681407E+01	1.409744E+02	6.898370E+01	7.829476E+01	2.269450E+00	1.119172E+02	3.180127E+02	2.396581747342E+08	1290487
18	5.106375E+03	1.893090E+02	4.898834E+01	1.291509E+02	6.796814E+01	7.773487E+01	4.160465E+01	1.124790E+02	3.478119E+02	2.396590991929E+08	2889014
19	7.472168E+02	1.868377E+02	4.879556E+01	1.334869E+02	6.783618E+01	7.843820E+01	4.035171E+01	1.130395E+02	3.498450E+02	2.396591083155E+08	2903409
20	5.836695E+02	1.814474E+02	4.865161E+01	1.422525E+02	6.672875E+01	7.627213E+01	3.548330E+02	1.099225E+02	3.188514E+02	2.396924843675E+08	11181733
21	8.121642E+02	1.816064E+02	4.582505E+01	1.455328E+02	6.927760E+01	7.904011E+01	4.119340E+01	1.126623E+02	2.903141E+00	2.396937279845E+08	2004100
22	1.462864E+02	1.824575E+02	4.912804E+01	1.402244E+02	6.657982E+01	3.083014E+01	2.587232E+02	6.557020E+01	1.626861E+01	2.396961748119E+08	6589035

LAT DATA FORMAT

- **spacecraft files** (aka housekeeping files):
  for each event, includes the energy, the sky arrival direction, the quality of the reconstructed event

Select	START	STOP	SC_POSITION	LAT_GEO	LON_GEO	RAD_GEO	RA_ZENITH	DEC_ZENITH	B_MCILWAIN	L_MCILWAIN	GEOMAG_LAT
	D	D	3E	E	E	D	E	E	E	E	E
All	s	s	m	deg	deg	m	deg	deg	Gauss	Earth_Radii	deg
Invert	Modify	Modify	Modify	Modify	Modify	Modify	Modify	Modify	Modify	Modify	Modify
1	2.395574174942E+08	2.395574466000E+08	Plot	1.844749E+01	-9.255068E+01	5.399130526349E+05	9.693066E+01	1.834127E+01	3.138191E+00	1.429734E+00	3.324647E+01
2	2.395574466000E+08	2.395574766000E+08	Plot	1.786626E+01	-9.084282E+01	5.400102692170E+05	9.876013E+01	1.776295E+01	3.064357E+00	1.423360E+00	3.305048E+01
3	2.395574766000E+08	2.395575066000E+08	Plot	1.724941E+01	-8.909514E+01	5.401241736156E+05	1.006332E+02	1.714921E+01	2.984627E+00	1.416692E+00	3.284293E+01
4	2.395575066000E+08	2.395575366000E+08	Plot	1.661528E+01	-8.736010E+01	5.402510991608E+05	1.024935E+02	1.651834E+01	2.900238E+00	1.408996E+00	3.260005E+01
5	2.395575366000E+08	2.395575666000E+08	Plot	1.596466E+01	-8.563747E+01	5.403894299848E+05	1.043415E+02	1.587111E+01	2.810311E+00	1.401272E+00	3.235264E+01
6	2.395575666000E+08	2.395575966000E+08	Plot	1.529835E+01	-8.392696E+01	5.405426559357E+05	1.061774E+02	1.520832E+01	2.716681E+00	1.392566E+00	3.206923E+01
7	2.395575966000E+08	2.395576266000E+08	Plot	1.461712E+01	-8.222823E+01	5.407080061907E+05	1.080014E+02	1.453074E+01	2.608127E+00	1.383829E+00	3.177983E+01
8	2.395576266000E+08	2.395576566000E+08	Plot	1.392177E+01	-8.054092E+01	5.408898597805E+05	1.098141E+02	1.383917E+01	2.520987E+00	1.374233E+00	3.145602E+01
9	2.395576566000E+08	2.395576866000E+08	Plot	1.321308E+01	-7.886463E+01	5.410834016968E+05	1.116157E+02	1.313437E+01	2.420614E+00	1.364511E+00	3.112139E+01
10	2.395576866000E+08	2.395577166000E+08	Plot	1.249183E+01	-7.719890E+01	5.412909276185E+05	1.134068E+02	1.241715E+01	2.318201E+00	1.354345E+00	3.076402E+01
11	2.395577166000E+08	2.395577466000E+08	Plot	1.175882E+01	-7.554327E+01	5.415124945196E+05	1.151878E+02	1.168826E+01	2.217724E+00	1.343371E+00	3.036938E+01
12	2.395577466000E+08	2.395577766000E+08	Plot	1.101480E+01	-7.389725E+01	5.417498436402E+05	1.169591E+02	1.094848E+01	2.116858E+00	1.332149E+00	2.995587E+01
13	2.395577766000E+08	2.395578066000E+08	Plot	1.026057E+01	-7.226027E+01	5.419994420083E+05	1.187214E+02	1.019859E+01	2.017124E+00	1.320367E+00	2.951028E+01
14	2.395578066000E+08	2.395578366000E+08	Plot	9.496881E+00	-7.063181E+01	5.422622995504E+05	1.204753E+02	9.439344E+00	1.919298E+00	1.307884E+00	2.902472E+01
15	2.395578366000E+08	2.395578666000E+08	Plot	8.724513E+00	-6.901128E+01	5.425414003989E+05	1.222211E+02	8.671507E+00	1.823221E+00	1.294480E+00	2.848694E+01
16	2.395578666000E+08	2.395578966000E+08	Plot	7.944216E+00	-6.739810E+01	5.428319375541E+05	1.239596E+02	7.895826E+00	1.731516E+00	1.280929E+00	2.792483E+01
17	2.395578966000E+08	2.395579266000E+08	Plot	7.156761E+00	-6.579165E+01	5.431382326489E+05	1.256914E+02	7.113063E+00	1.642843E+00	1.266081E+00	2.728608E+01
18	2.395579266000E+08	2.395579566000E+08	Plot	6.362885E+00	-6.419132E+01	5.434570608616E+05	1.274171E+02	6.323952E+00	1.557904E+00	1.251457E+00	2.663170E+01
19	2.395579566000E+08	2.395579866000E+08	Plot	5.563341E+00	-6.259646E+01	5.437888100188E+05	1.291373E+02	5.529237E+00	1.478563E+00	1.236706E+00	2.594403E+01
20	2.395579866000E+08	2.395580166000E+08	Plot	4.758880E+00	-6.100642E+01	5.441360150658E+05	1.308527E+02	4.729660E+00	1.404279E+00	1.221925E+00	2.522461E+01
21	2.395580166000E+08	2.395580466000E+08	Plot	3.950237E+00	-5.942054E+01	5.444953555272E+05	1.325639E+02	3.925949E+00	1.335575E+00	1.207762E+00	2.450395E+01
22	2.395580466000E+08	2.395580690931E+08	Plot	3.138157E+00	-5.783817E+01	5.448677722007E+05	1.342716E+02	3.118841E+00	1.273103E+00	1.194659E+00	2.380718E+01

LAT DATA FORMAT

LAT events are based on their probability of being photons (event class)

Standard Hierarchy for LAT Event Classes				
Event Class	**evclass**	**Photon File**	**Extended File**	**Description**
P8R3_TRANSIENT020	16		X	Transient event class with background rate equal to two times the A10 IGRB reference spectrum.
P8R3_TRANSIENT010	64		X	Transient event class with background rate equal to one times the A10 IGRB reference spectrum.
P8R3_SOURCE	128	X	X	This event class has a residual background rate that is comparable to P7REP_SOURCE. This is the recommended class for most analyses and provides good sensitivity for analysis of point sources and moderately extended sources.
P8R3_CLEAN	256	X	X	This class is identical to SOURCE below 3 GeV. Above 3 GeV it has a 1.3-2 times lower background rate than SOURCE and is slightly more sensitive to hard spectrum sources at high galactic latitudes.
P8R3_ULTRACLEAN	512	X	X	This class has a background rate very similar to ULTRACLEANVETO.
P8R3_ULTRACLEANVETO	1024	X	X	This is the cleanest Pass 8 event class. Its background rate is 15-20% lower than the background rate of SOURCE class below 10 GeV, and 50% lower at 200 GeV. This class is recommended to check for CR-induced systematics as well as for studies of diffuse emission that require low levels of CR contamination.
P8R3_SOURCEVETO	2048	X	X	This class has the same background rate than the SOURCE class background rate up to 10 GeV but, above 50 GeV, its background rate is the same as the ULTRACLEANVETO one while having 15% more acceptance.

LAT DATA FORMAT

Each event class was partitioned in two event types (front and back) depending on the location of the tracker layer where the photon-to-pair occurred. **Front-converted events have intrinsically better angular resolution than back-converted ones.**

Conversion Type Partition		
Event Type	**evtype**	**Description**
FRONT	1	Events converting in the Front-section of the Tracker. Equivalent to convtype=0.
BACK	2	Events converting in the Back-section of the Tracker. Equivalent to convtype=1.

ZENITH ANGLE SELECTION

Important to avoid gamma-ray produced by CRs interacting with the Earth's atmosphere

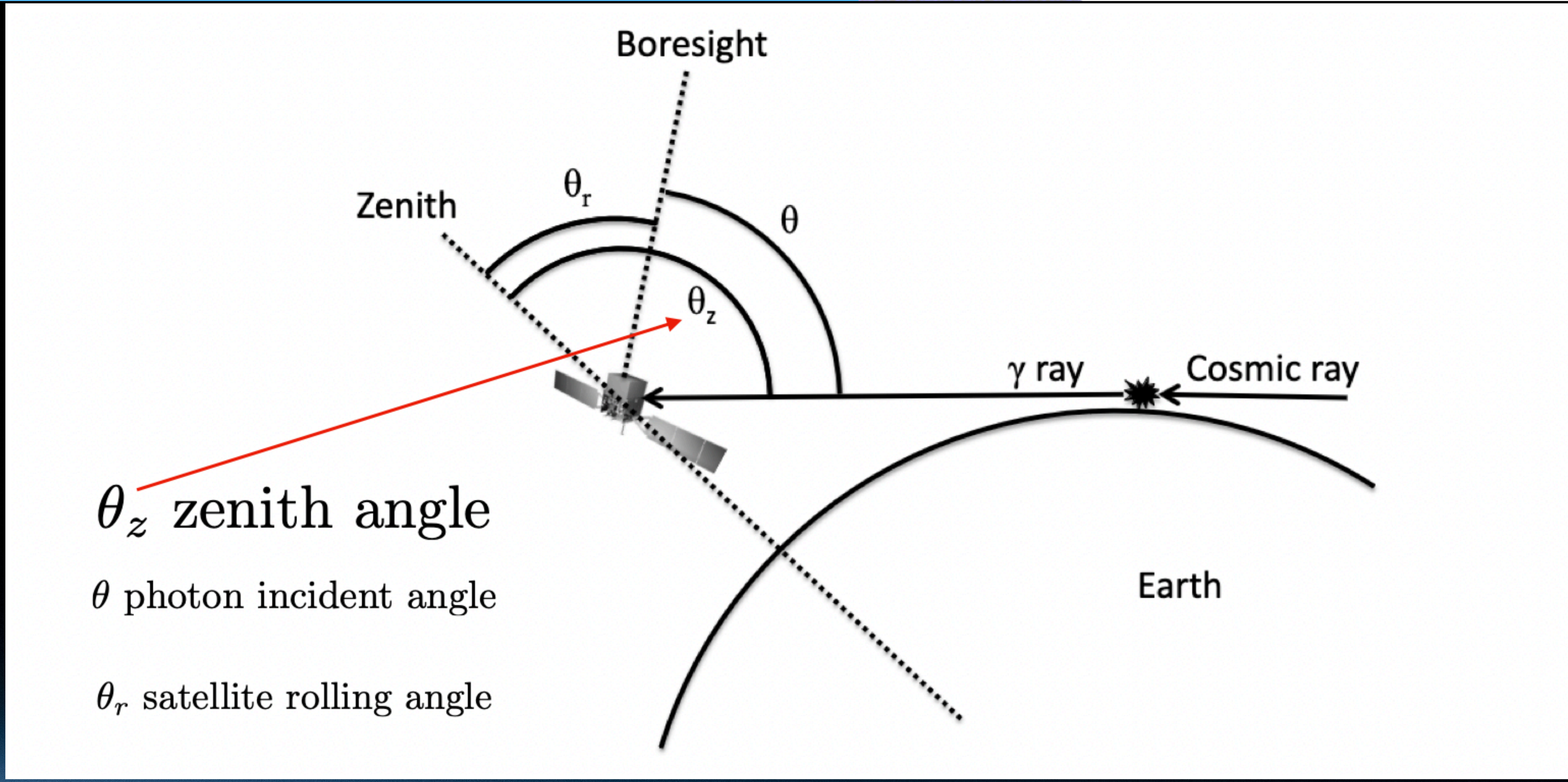

IMAGE

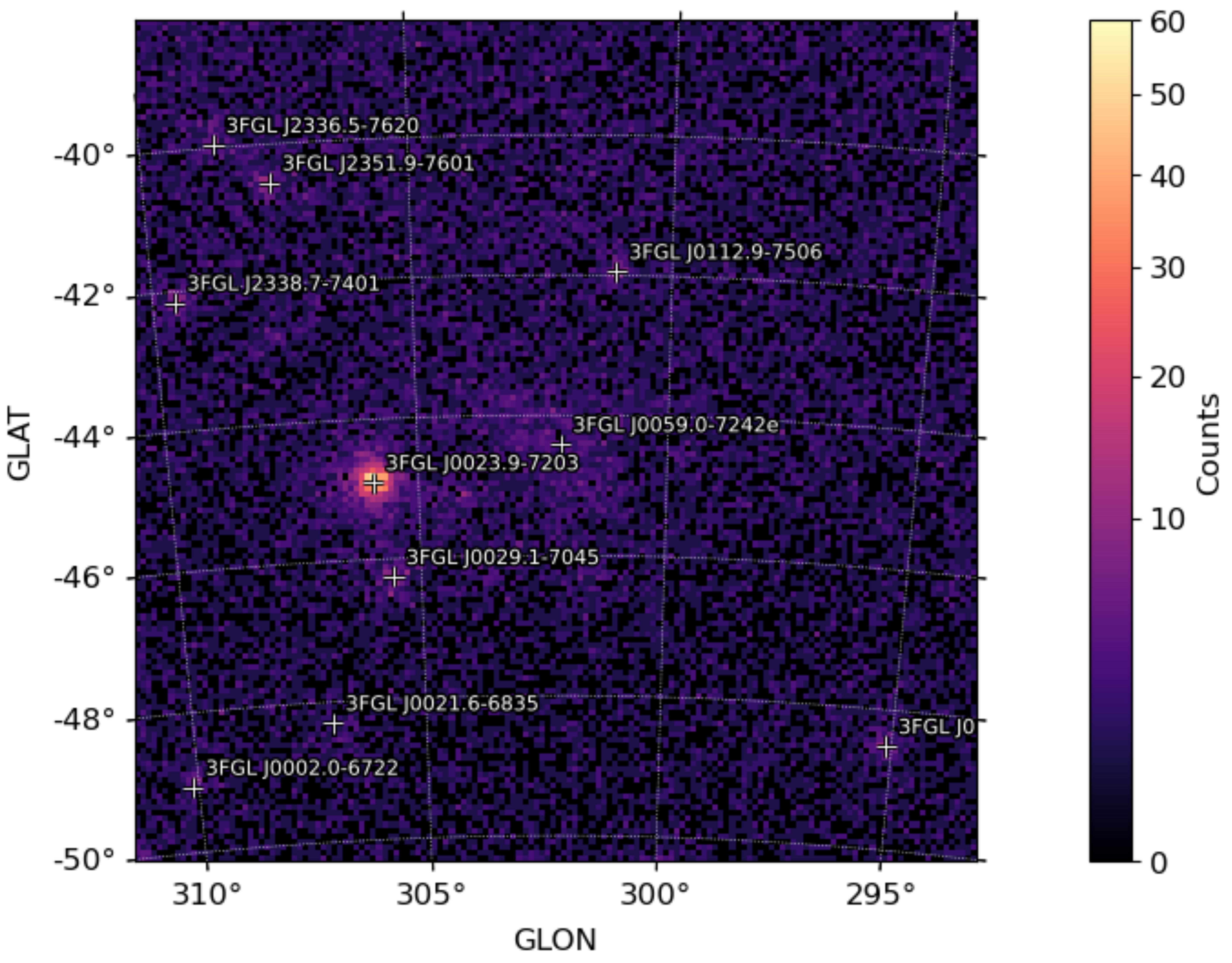

Counts map is a 2D representation of the studied region. In binned analysis (hereafter the assumed analysis) the events are binned into user specified squared pixels.

A 3D count cube (spatial+energy) is a set of count maps produced at different energy bins.

The analysed region is called Region of Interest (RoI). Typical RoI has a radius of 10°-20°, centred on the source of interest, and including all sources nearby the target and the background


IMAGE
Isotropic background
dominated by unresolved point-like sources
Galactic background
dominated by CRs interactions in the Galactic plane

IRF: Instrument Response Function

Each event class and event type selection (s) has its own IRFs

$$R = A_{\rm eff} \times {\rm PSF} \times D$$

1. Effective area $A_{\rm eff}\left(E, \hat{v}, s\right)$
   the product of the cross-sectional geometrical collection area, gamma-ray conversion probability, and the efficiency of a given event selection (denoted by s) for a gamma-ray photon with energy E and direction $\hat{v}$ in the LAT frame

2. Point-spread function $P\left(\hat{v}'; E, \hat{v}, s\right)$
   the probability density to reconstruct an incident direction $\hat{v}'$ for a gamma-ray with $\left(E, \hat{v}\right)$ in the event selection s

3. Energy Dispersion $D\left(E'; E, \hat{v}, s\right)$
   the probability density to measure an event energy E' for a gamma-ray with $\left(E, \hat{v}\right)$ in the event selection s

EFFECTIVE AREA

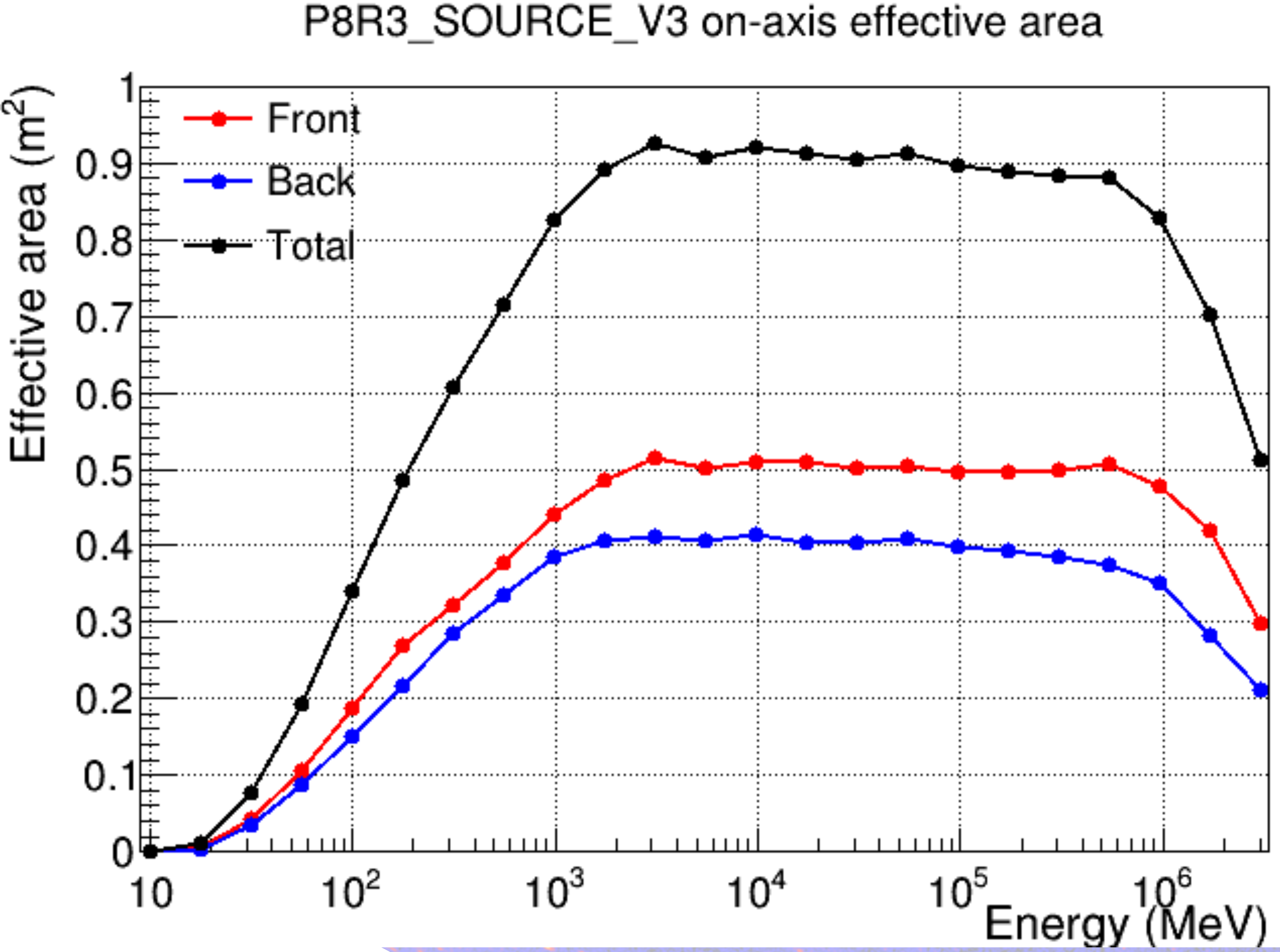

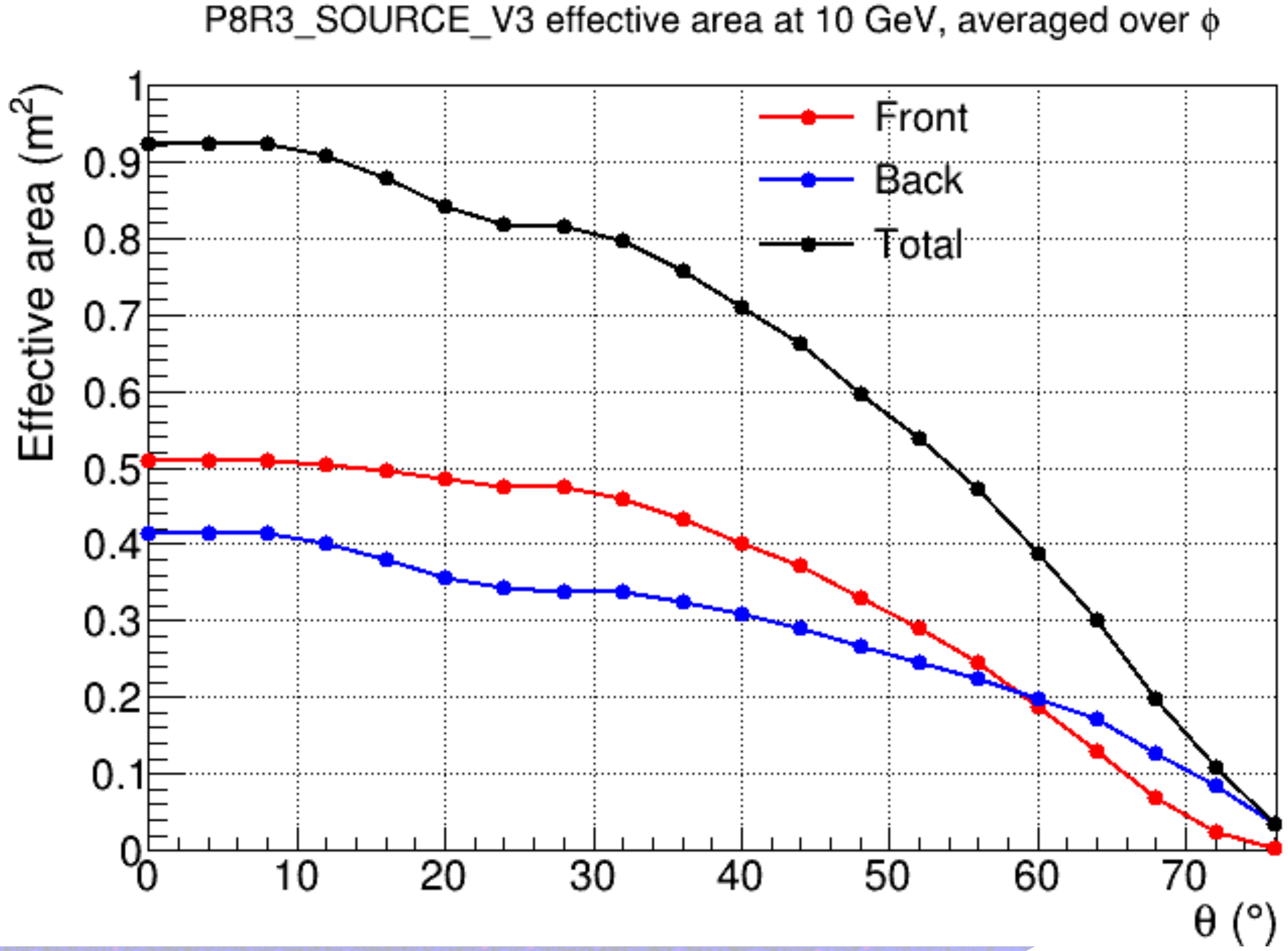

PSF

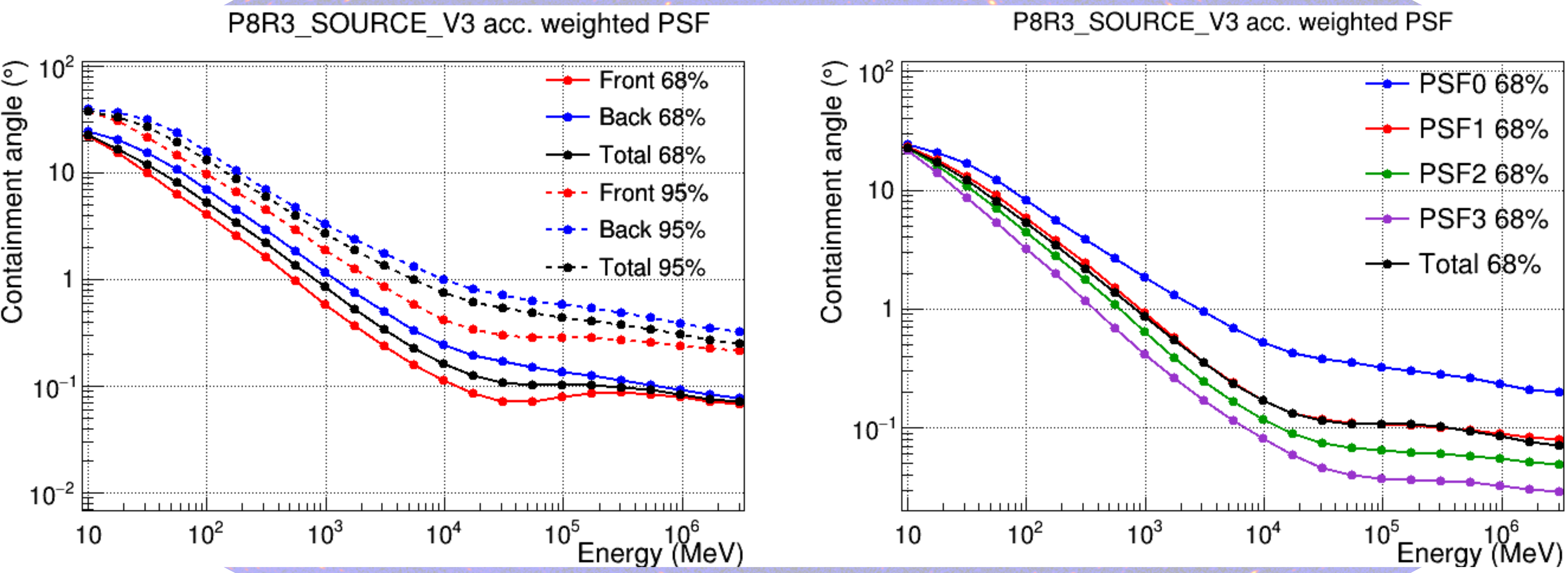
P8R3_SOURCE_V3 acc. weighted PSF
Containment angle (°)
Energy (MeV)
Front 68%
Back 68%
Total 68%
Front 95%
Back 95%
Total 95%
P8R3_SOURCE_V3 acc. weighted PSF
Containment angle (°)
Energy (MeV)
PSF0 68%
PSF1 68%
PSF2 68%
PSF3 68%
Total 68%

ENERGY RESOLUTION

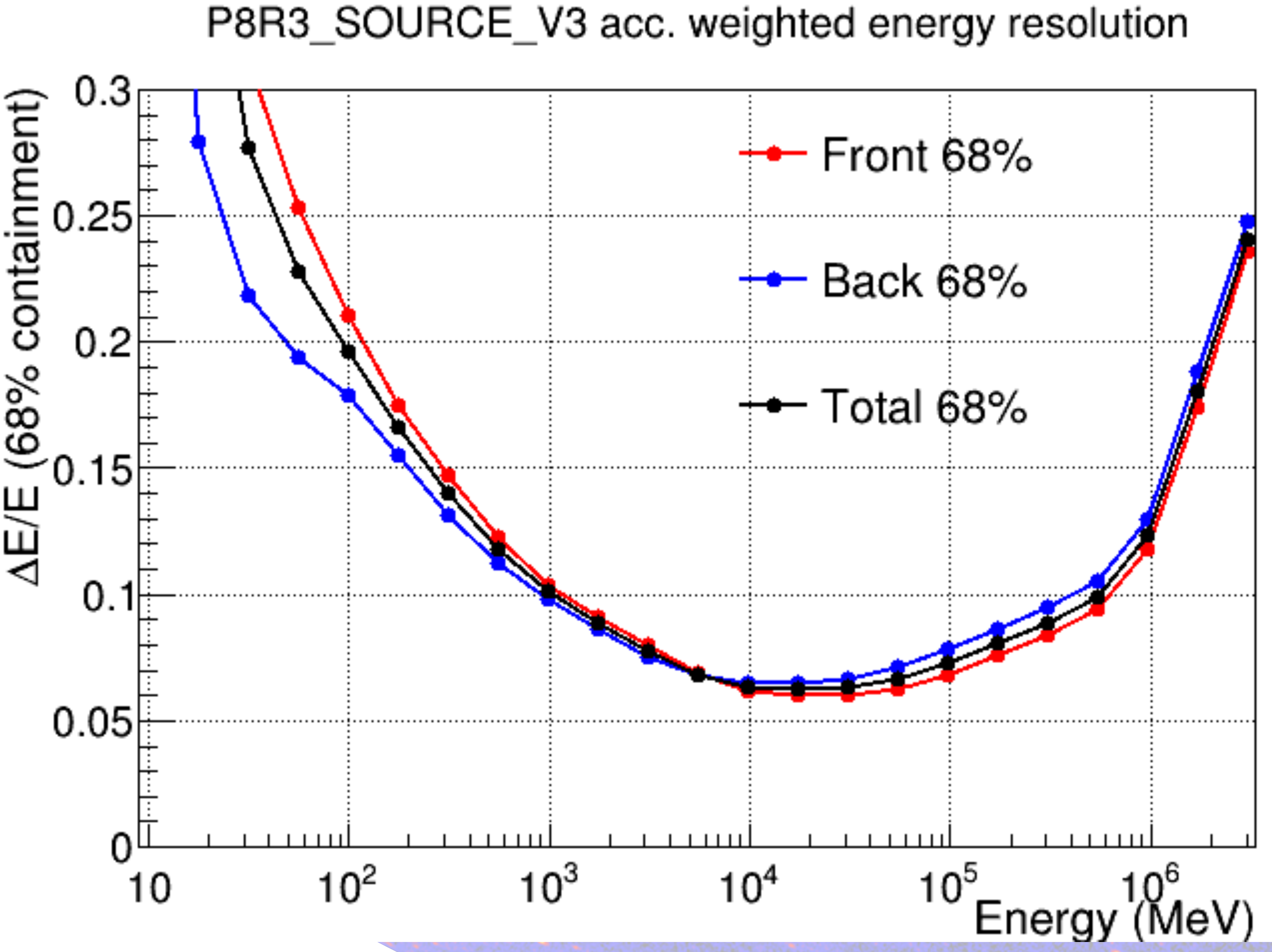

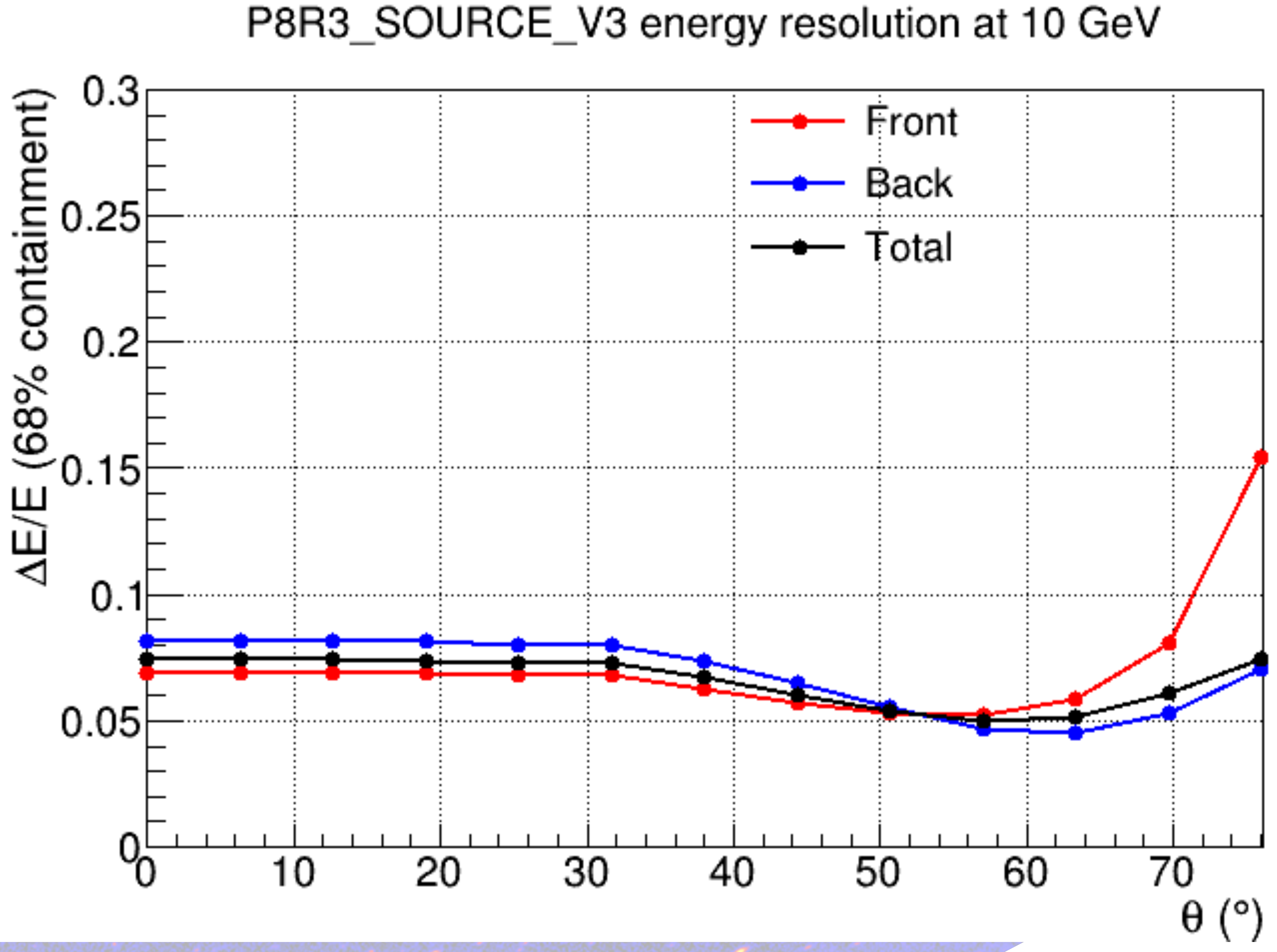

STATISTICS

Because of

- the paucity of the events
- the large errors associated with detecting gamma-rays
- the brightness of the background

THE METHOD OF MAXIMUM LIKELIHOOD

STATISTICS

x r.v. distributed according to a p.d.f. $f(x;\theta)$

The functional form $f(x;\theta)$ is known but θ is known.

Likelihood function:

$$\mathscr{L}(\theta) = \prod_{i=1}^{n} f\left(x_i;\theta\right)$$

Maximum likelihood estimator

$$\frac{\partial \mathscr{L}}{\partial \theta_i} = 0, \quad i = i, \ldots, m$$

STATISTICS

The source model is considered as

$$S\left(E,\hat{p},t\right) = \sum_{i} s_i\left(E_i,t\right)\delta\left(\hat{p}-\hat{p}_i\right) + S_G\left(E,\hat{p}\right) + S_{eg}\left(E,\hat{p}\right) + \sum_{l} S_l\left(E_l,\hat{p},t\right)$$

STATISTICS

The source model is considered as

$$S\left(E,\hat{p},t\right)=\sum_i s_i\left(E_i,t\right)\delta\left(\hat{p}-\hat{p}_i\right)+S_G\left(E,\hat{p}\right)+S_{eg}\left(E,\hat{p}\right)+\sum_l S_l\left(E_l,\hat{p},t\right)$$

STATISTICS

The source model is considered as

$$S\left(E,\hat{p},t\right) = \sum_i s_i\left(E_i,t\right)\delta\left(\hat{p}-\hat{p}_i\right) + S_G\left(E,\hat{p}\right) + S_{eg}\left(E,\hat{p}\right) + \sum_l S_l\left(E_l,\hat{p},t\right)$$

Galactic & Extragalactic backgrounds

STATISTICS

The source model is considered as

$$S\left(E,\hat{p},t\right) = \sum_i s_i\left(E_i,t\right)\delta\left(\hat{p}-\hat{p}_i\right) + S_G\left(E,\hat{p}\right) + S_{eg}\left(E,\hat{p}\right) + \sum_l S_l\left(E_l,\hat{p},t\right)$$

other sources

STATISTICS

The source model is considered as

$$S\left(E,\hat{p},t\right) = \sum_i s_i\left(E_i,t\right)\delta\left(\hat{p}-\hat{p}_i\right) + S_G\left(E,\hat{p}\right) + S_{eg}\left(E,\hat{p}\right) + \sum_l S_l\left(E_l,\hat{p},t\right)$$

The model is then folded with the IRF to obtain the predicted counts in the measured quantity space $\left(E',\hat{p}',t'\right)$

$$M\left(E',\hat{p}',t\right) = \int_{\mathrm{SR}} dE\, d\hat{p}\, R\left(E',\hat{p}',t;E,\hat{p}\right) S\left(E,\hat{p},t\right)$$

STATISTICS

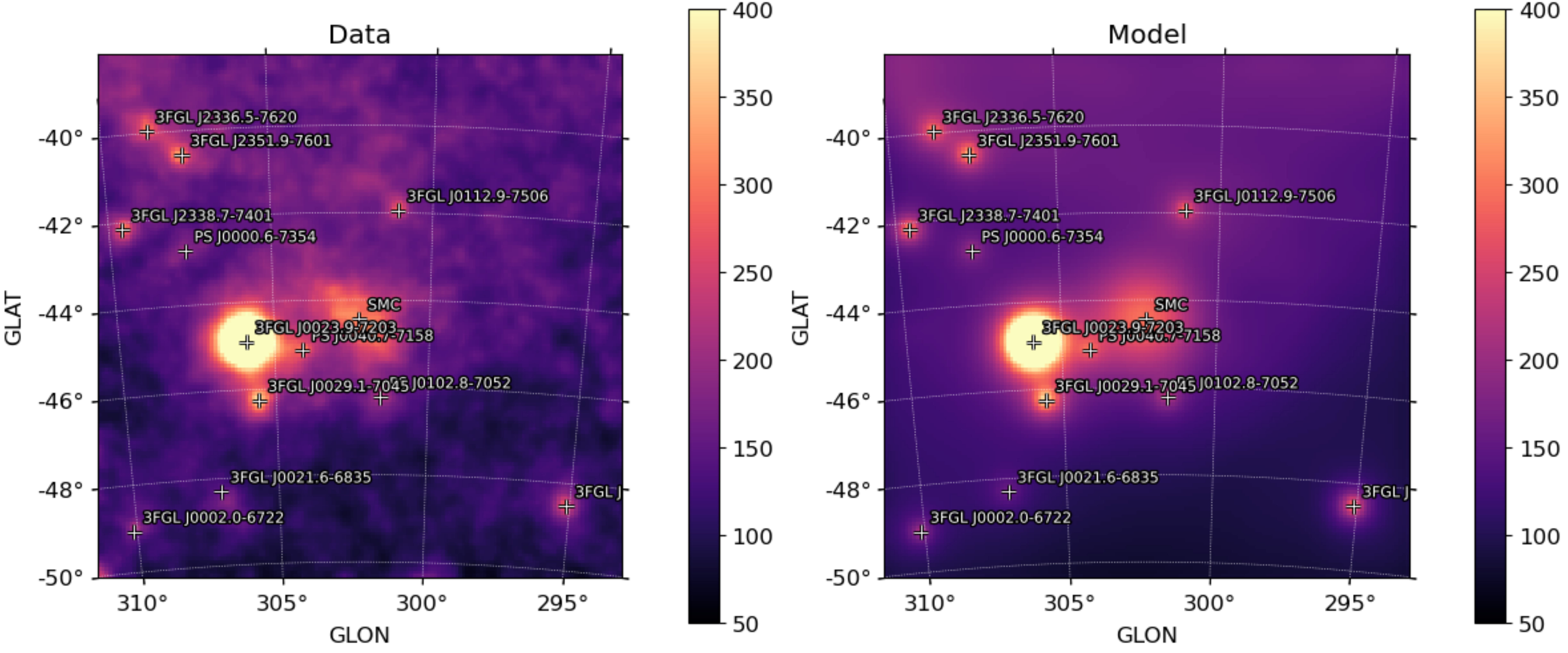
Data
Model
3FGL J2336.5-7620
3FGL J2351.9-7601
3FGL J0112.9-7506
3FGL J2338.7-7401
PS J0000.6-7354
SMC
3FGL J0023.9-7203
3FGL J0029.1-7045
3FGL J0021.6-6835
3FGL J0002.0-6722
GLAT
GLON
-40°
-42°
-44°
-46°
-48°
-50°
310°
305°
300°
295°
400
350
300
250
200
150
100
50

STATISTICS

The number of counts in each bin/pixel is small and it is well described by a Poisson distribution

$$p_\lambda(n) = \frac{\lambda^n}{n!} e^{-\lambda}$$

λ average # of events

n # of events in each bin

STATISTICS

$\mathscr{L}$ is the product of the probabilities of observing n_k counts in each bin (k) when the number of counts predicted by the model is m_k

$$\mathscr{L} = \prod_k \frac{m_k^{n_k} e^{-m_k}}{n_k!} = \prod_k e^{-m_k} \prod_k \frac{m_k^{n_k}}{n!} = e^{-N_{\mathrm{pred}}} \frac{m_k^{n_k}}{n!}$$

$$\ln \mathscr{L} = -N_{\mathrm{pred}} + \sum_k n_k \ln\left(m_k\right) - \ln\left(n!\right)$$

This does not depend on the model.
It can be neglected.

STATISTICS

As a standalone value, $\mathscr{L}$ is meaningless!

A test statistics (TS) is defined as

$$\mathrm{TS} = -2\ln\left(\frac{\mathscr{L}_{\mathrm{null}}}{\mathscr{L}_{\mathrm{src}}}\right)$$

where $\mathscr{L}_{\mathrm{null}}$ and $\mathscr{L}_{\mathrm{src}}$ are the maximum likelihood values under the null (no additional sources) and alternative (additional source) hypothesis.

In the limit of a large number of counts, Wilks' theorem states that the TS for the null hypothesis is asymptotically distributed as a χ^2_n distribution, where n is the number of the parameters characterising the additional source

STATISTICS

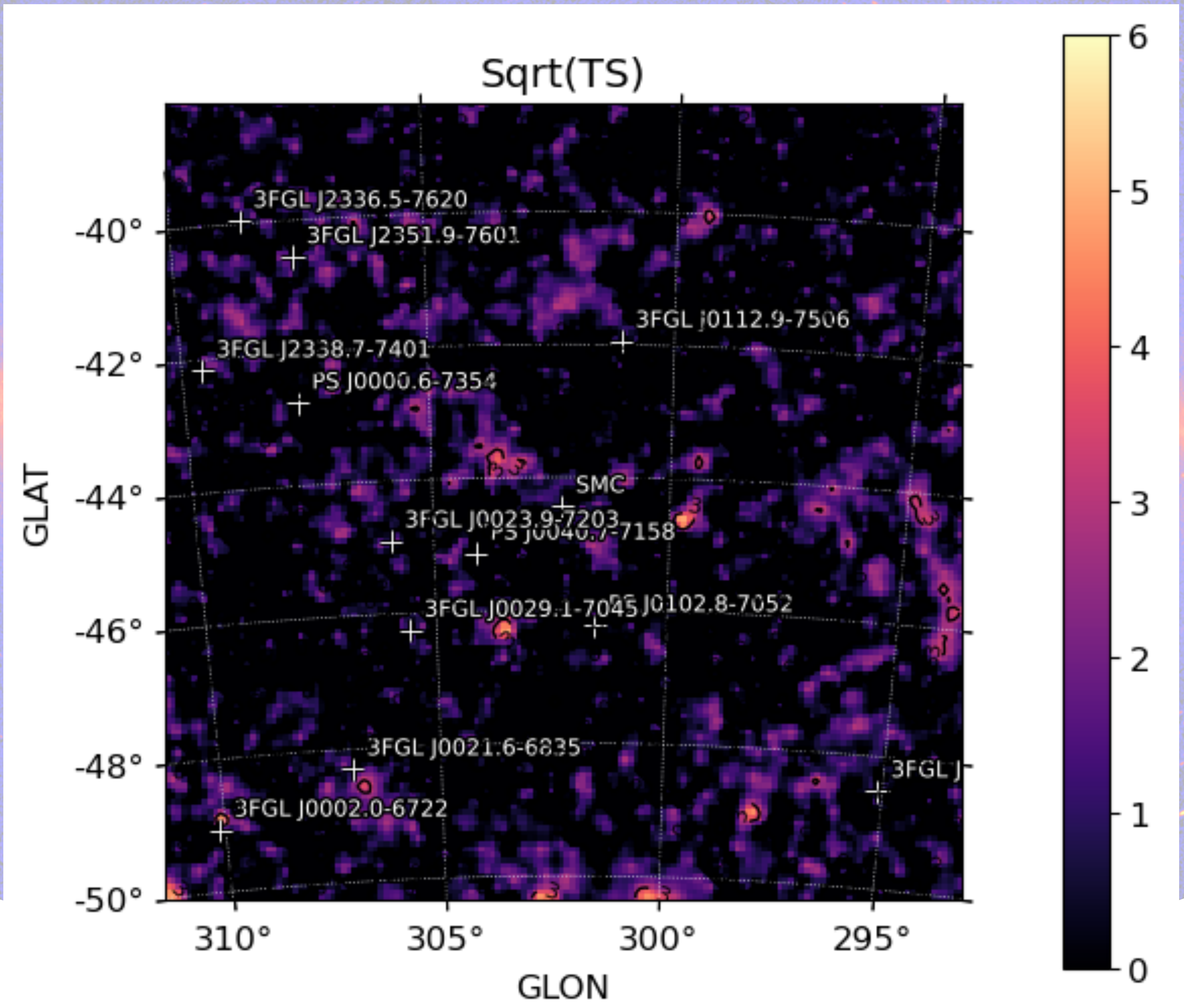
Sqrt(TS)
3FGL J2336.5-7620
3FGL J2351.9-7601
3FGL J0112.9-7506
3FGL J2338.7-7401
PS J0000.6-7354
SMC
3FGL J0023.9-7203
PS J0040.7-7158
3FGL J0029.1-7045
PS J0102.8-7052
3FGL J0021.6-6835
3FGL J0002.0-6722
3FGL J
-40°
-42°
-44°
-46°
-48°
-50°
310°
305°
300°
295°
GLAT
GLON
0
1
2
3
4
5
6

STATISTICS

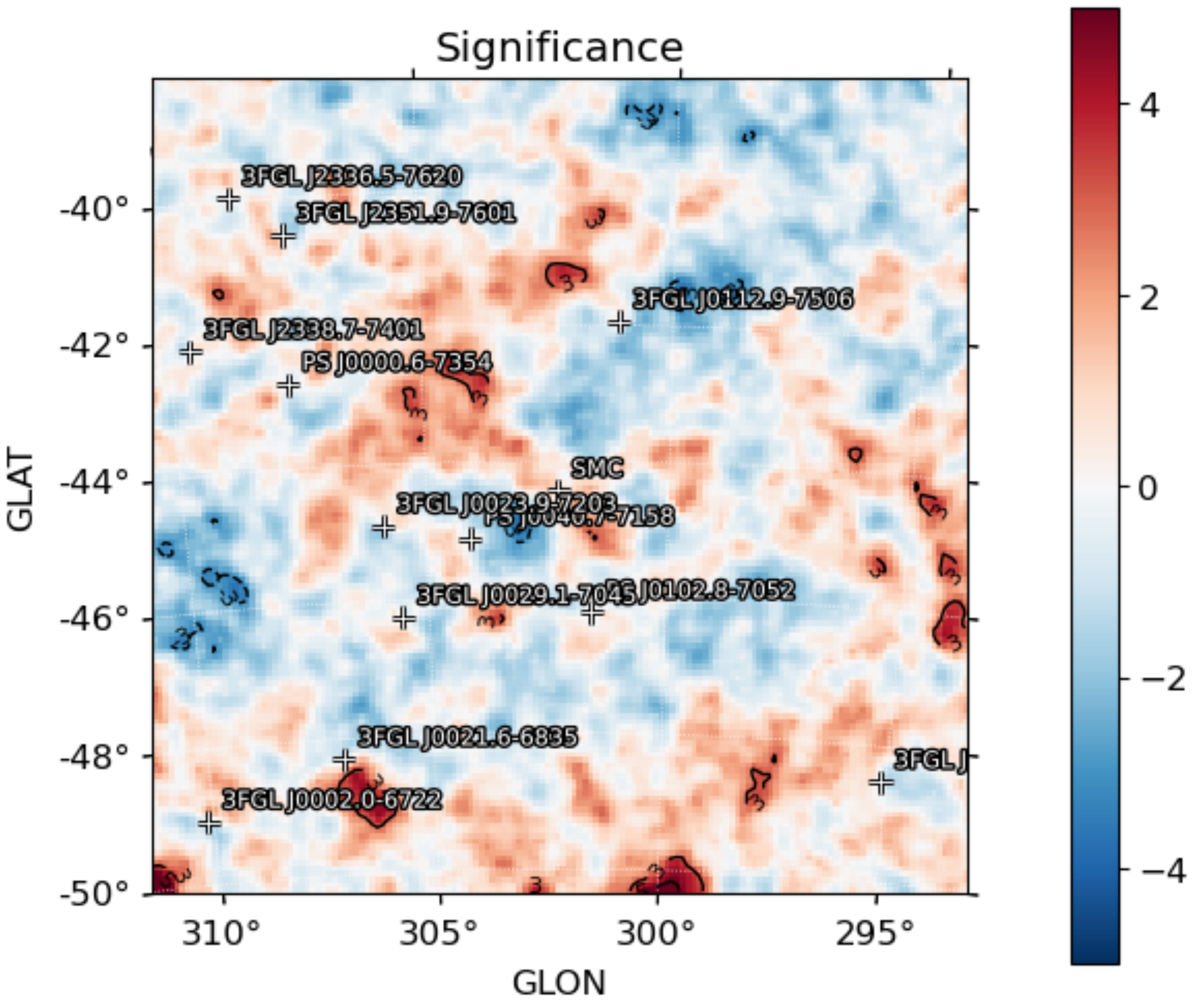
Significance
3FGL J2336.5-7620
3FGL J2351.9-7601
3FGL J0112.9-7506
3FGL J2338.7-7401
PS J0000.6-7354
SMC
3FGL J0023.9-7203
PS J0040.7-7158
3FGL J0029.1-7045
PS J0102.8-7052
3FGL J0021.6-6835
3FGL J0002.0-6722
3FGL J
GLAT
GLON
-40°
-42°
-44°
-46°
-48°
-50°
310°
305°
300°
295°
4
2
0
−2
−4

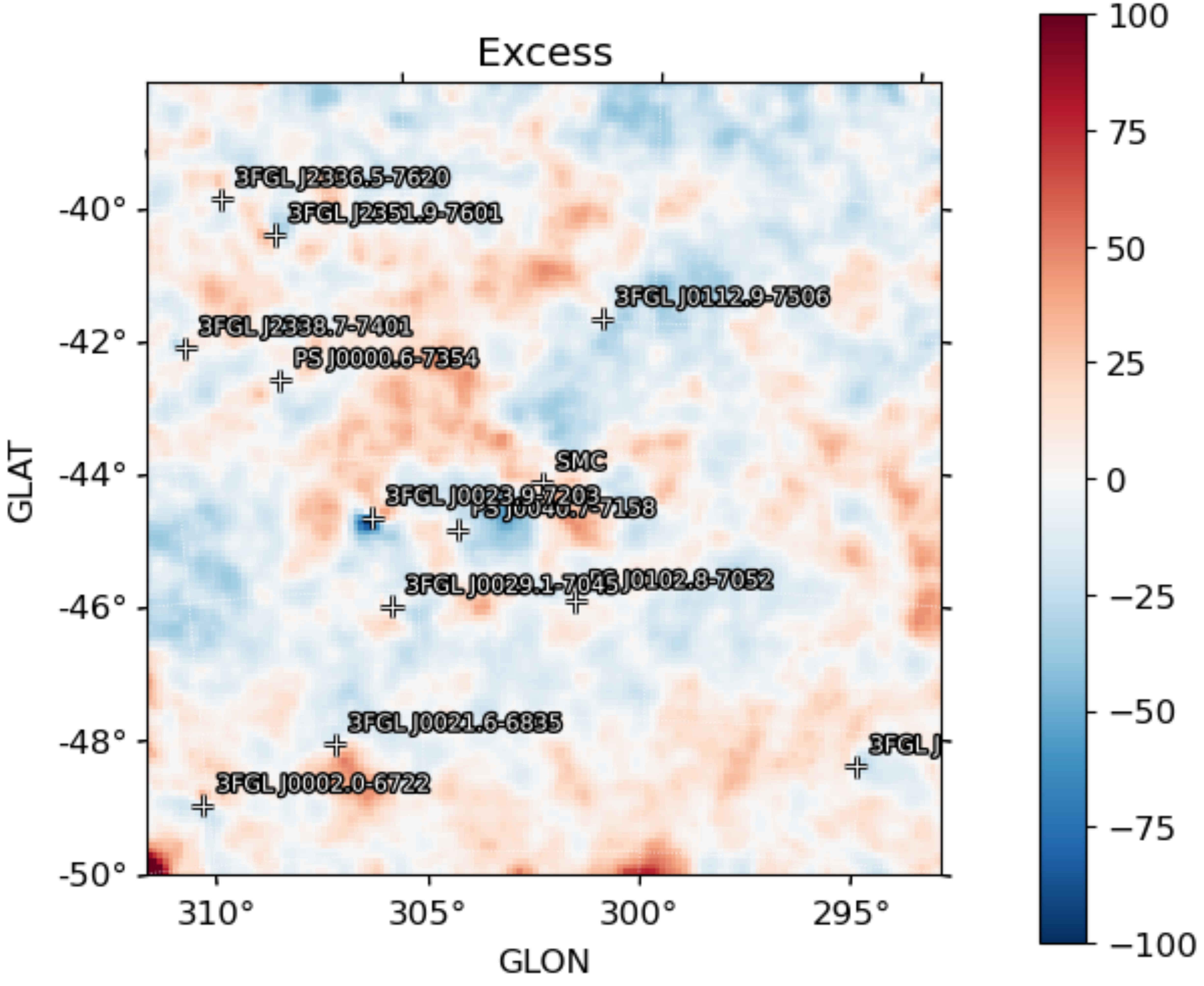
Excess
3FGL J2336.5-7620
3FGL J2351.9-7601
3FGL J0112.9-7506
3FGL J2338.7-7401
PS J0000.6-7354
SMC
3FGL J0023.9-7203
PS J0040.7-7158
3FGL J0029.1-7045
PS J0102.8-7052
3FGL J0021.6-6835
3FGL J0002.0-6722
3FGL J
GLAT
GLON
-40°
-42°
-44°
-46°
-48°
-50°
310°
305°
300°
295°
100
75
50
25
0
−25
−50
−75
−100

STATISTICS

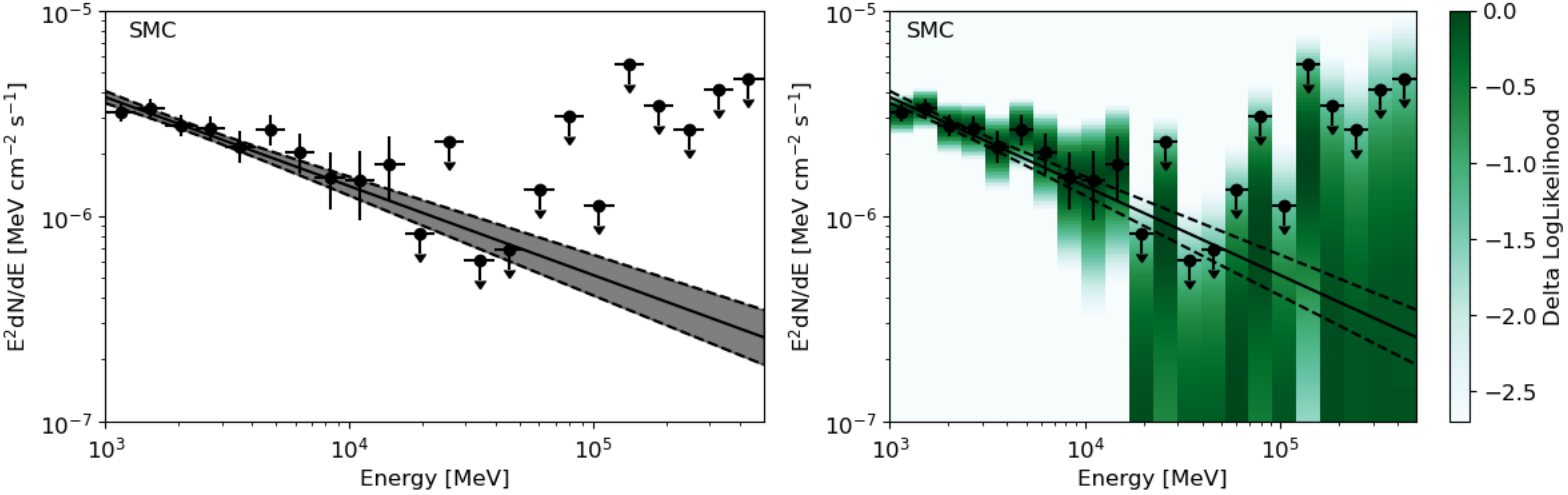

SMC
10^{-5}
10^{-6}
10^{-7}
E^2dN/dE [MeV cm^{-2} s^{-1}]
10^3
10^4
10^5
Energy [MeV]
SMC
Delta LogLikelihood
0.0
−0.5
−1.0
−1.5
−2.0
−2.5

LC and VARIABILITY

A light curve is produced by dividing the data into time bins and applying the likelihood analysis procedure to each bin

To test the variability of a source, we define a $\mathrm{TS_{var}}$ index, defined as

$$\mathrm{TS_{var}} \simeq 2 \sum_i \ln \left[\frac{\mathscr{L}_i\left(F_i\right)}{\mathscr{L}_i\left(F_{\mathrm{glob}}\right)} \right]$$

- $\mathscr{L}_i\left(F_{\mathrm{glob}}\right)$ is the likelihood obtained in the fit over the total time
- $\mathscr{L}_i\left(F_i\right)$ is the likelihood obtained in each interval by fixing the spectral parameters and adjusting the normalization
- $\mathrm{TS_{var}}$ is distributed as a χ^2_{n-1}, where n is the number of time bins

CTAO


Particle
Shower
~ 10 km
At 100 GeV
~ 10 Photons/m2
(300 – 600 nm)
5 nsec
~ 120 m
Focal Plane

Alpha Configuration:

- CTAO-N (La Palma): 4 LSTs + 9 MSTs
- CTAO-S (Chile, Panaral): 14 MSTs + 37 SSTs (+2 LSTs + 5 SSTs by PNRR CTA+)

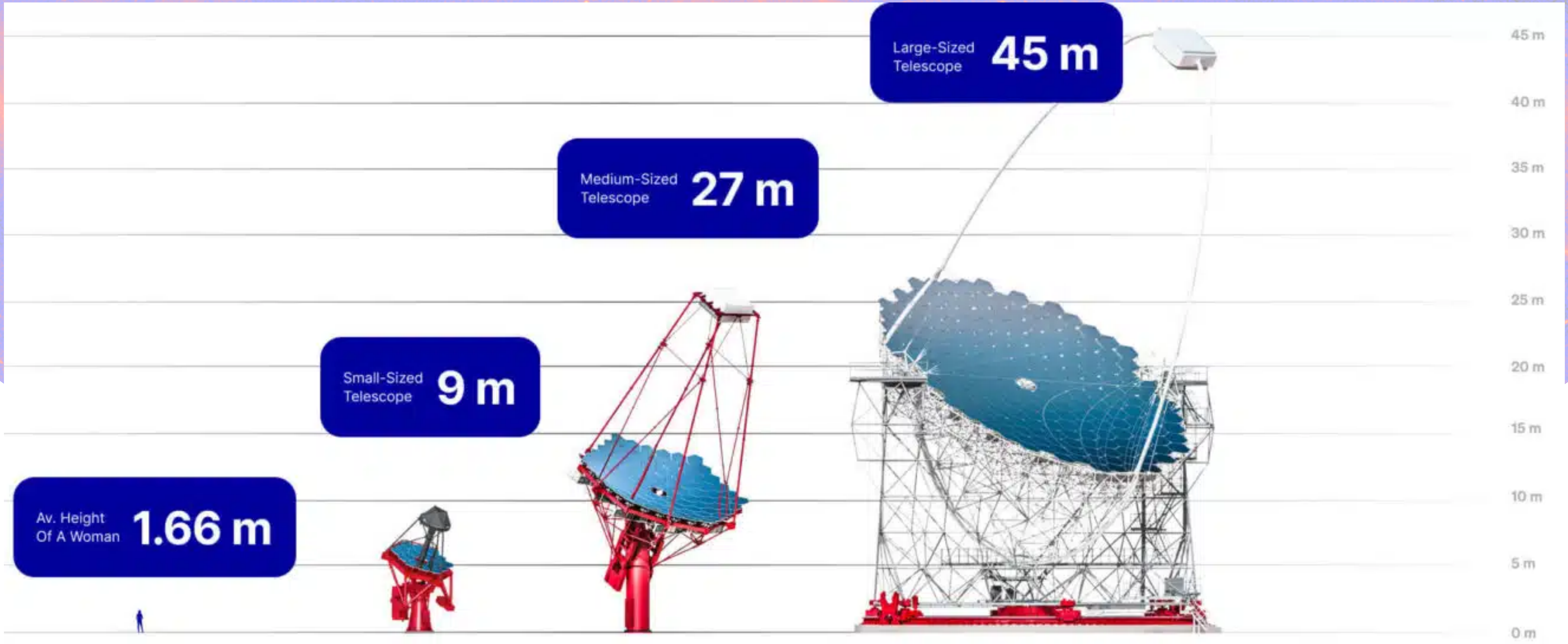

	Small-Sized Telescope (SST)
Energy range (in which sensitivity is optimized)	5 TeV – 300 TeV
Number of SST telescopes	37 (South)
Optical design	Modified Schwarzschild-Couder
Primary reflector diameter	4.3 m
Secondary reflector diameter	1.8 m
Effective mirror area (including shadowing)	>5 m^2
Focal length	2.15 m
Total weight	17.5 t
Field of view	8.8 deg
Number of pixels	2048
Pixel size (imaging)	0.16 deg
Photodetector type	SiPM
Telescope readout event rate (before array trigger)	600 Hz
Telescope data rates (readout of all pixels; before array trigger)	2.55 Gb/s
Positioning time to any point in the sky (>30° elevation)	70 s
Pointing precision	<7 arcseconds
Observable sky	Any astrophysical object with elevation > 24 degrees

	Medium-Sized Telescope (MST)
Energy range (in which sensitivity is optimized)	150 GeV – 5 TeV
Number of MST telescopes	14 (South) 9 (North)
Optical design	Modified Davies-Cotton
Reflector diameter	11.5 m
Effective mirror area (including shadowing)	88 m^2
Focal length	16 m
Total weight	89 t
Field of view (FlashCam / NectarCAM)	7.5 deg / 7.7 deg
Number of pixels (FlashCam / NectarCAM)	1764 / 1855
Pixel size (imaging)	0.17 deg
Photodetector type	PMT
Telescope readout event rate before array trigger (FlashCam / NectarCAM)	>6 kHz / >7.0 kHz
Telescope data rates (readout of all pixels; before array trigger)	12 Gb/s
Positioning time to any point in the sky (>30° elevation)	90 s
Pointing precision	<7 arcseconds
Observable sky	Any astrophysical object with elevation > 20 degrees

	Large-Sized Telescope (LST)
Energy range (in which sensitivity is optimized)	20 GeV – 150 GeV
Number of LST telescopes	4 (North)
Optical design	Parabolic
Primary reflector diameter	23.0 m
Effective mirror area (including shadowing)	370 m^2
Focal length	28 m
Total weight	103 t
Field of view	4.3 deg
Number of pixels	1855
Pixel size (imaging)	0.1 deg
Photodetector type	PMT
Telescope readout event rate after array trigger	>7.0 kHz
Telescope data rates (readout of all pixels; before array trigger)	24 Gb/s
Positioning time to any point in the sky (>30° elevation)	30 s
Pointing precision	<14 arcseconds
Observable sky	Any astrophysical object with elevation > 24 degrees

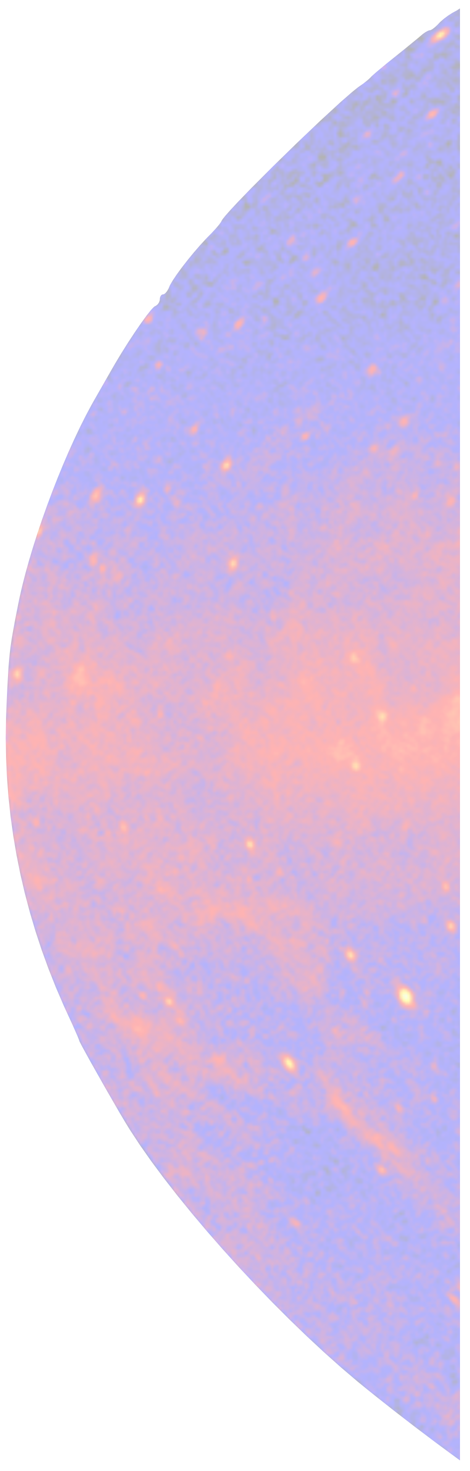

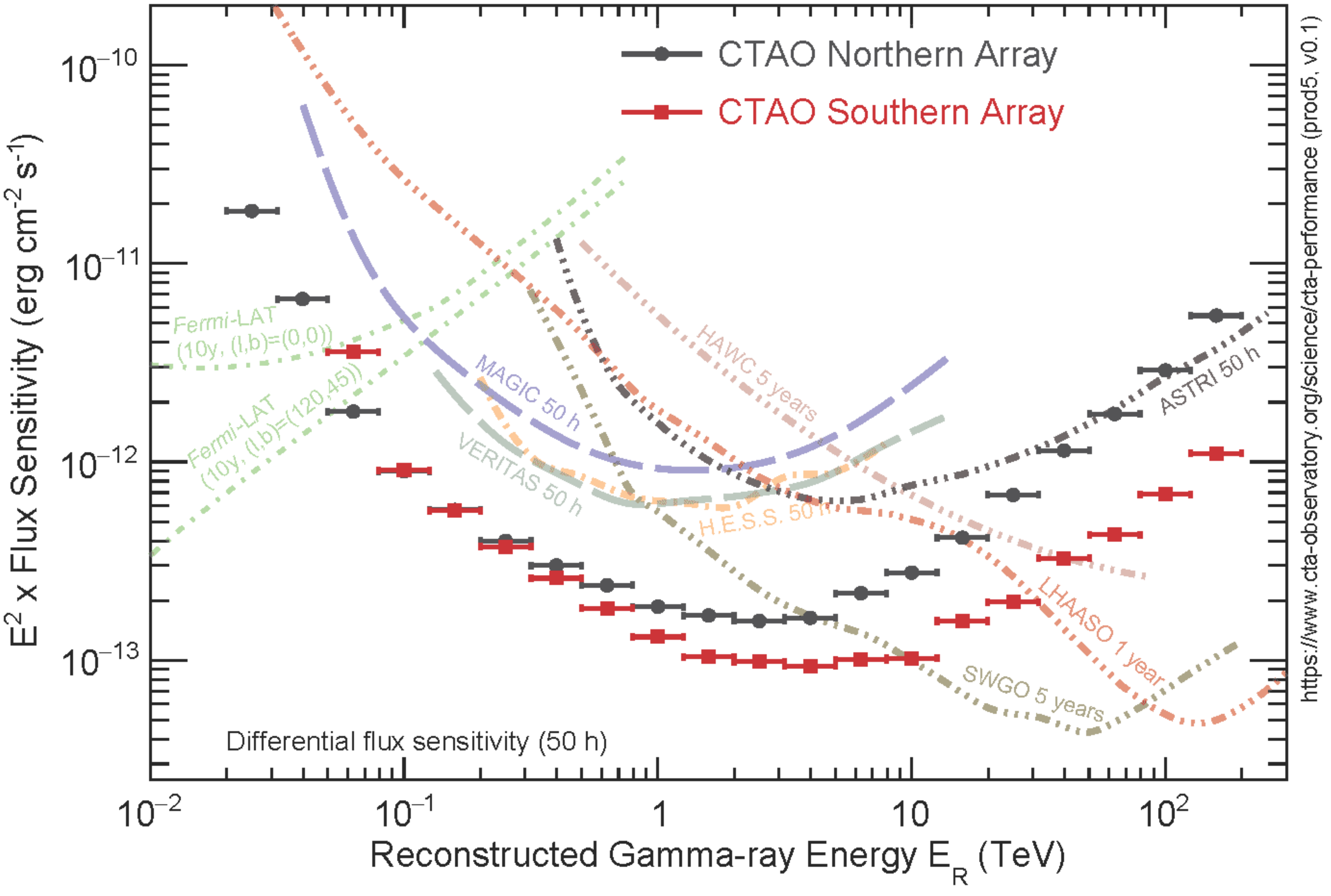
CTAO Northern Array
CTAO Southern Array
10^{-10}
10^{-11}
10^{-12}
10^{-13}
E^2 x Flux Sensitivity (erg cm^{-2} s^{-1})
Fermi-LAT (10y, (l,b)=(0,0))
Fermi-LAT (10y, (l,b)=(120,45))
MAGIC 50 h
VERITAS 50 h
H.E.S.S. 50 h
HAWC 5 years
LHAASO 1 year
SWGO 5 years
ASTRI 50 h
Differential flux sensitivity (50 h)
10^{-2}
10^{-1}
1
10
10^2
Reconstructed Gamma-ray Energy E_R (TeV)
https://www.cta-observatory.org/science/cta-performance (prod5, v0.1)

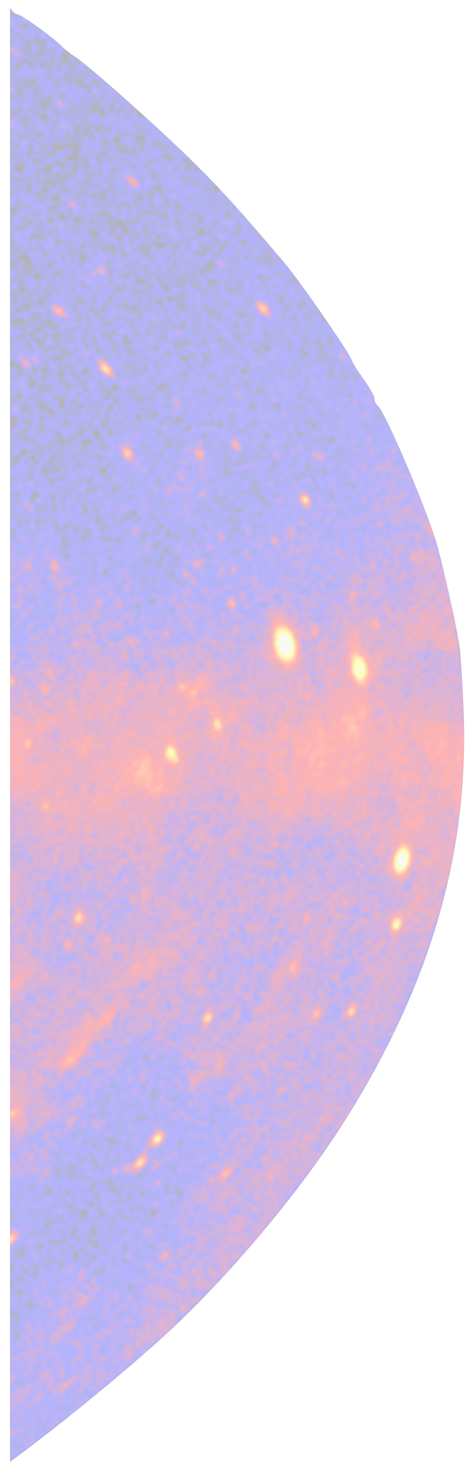

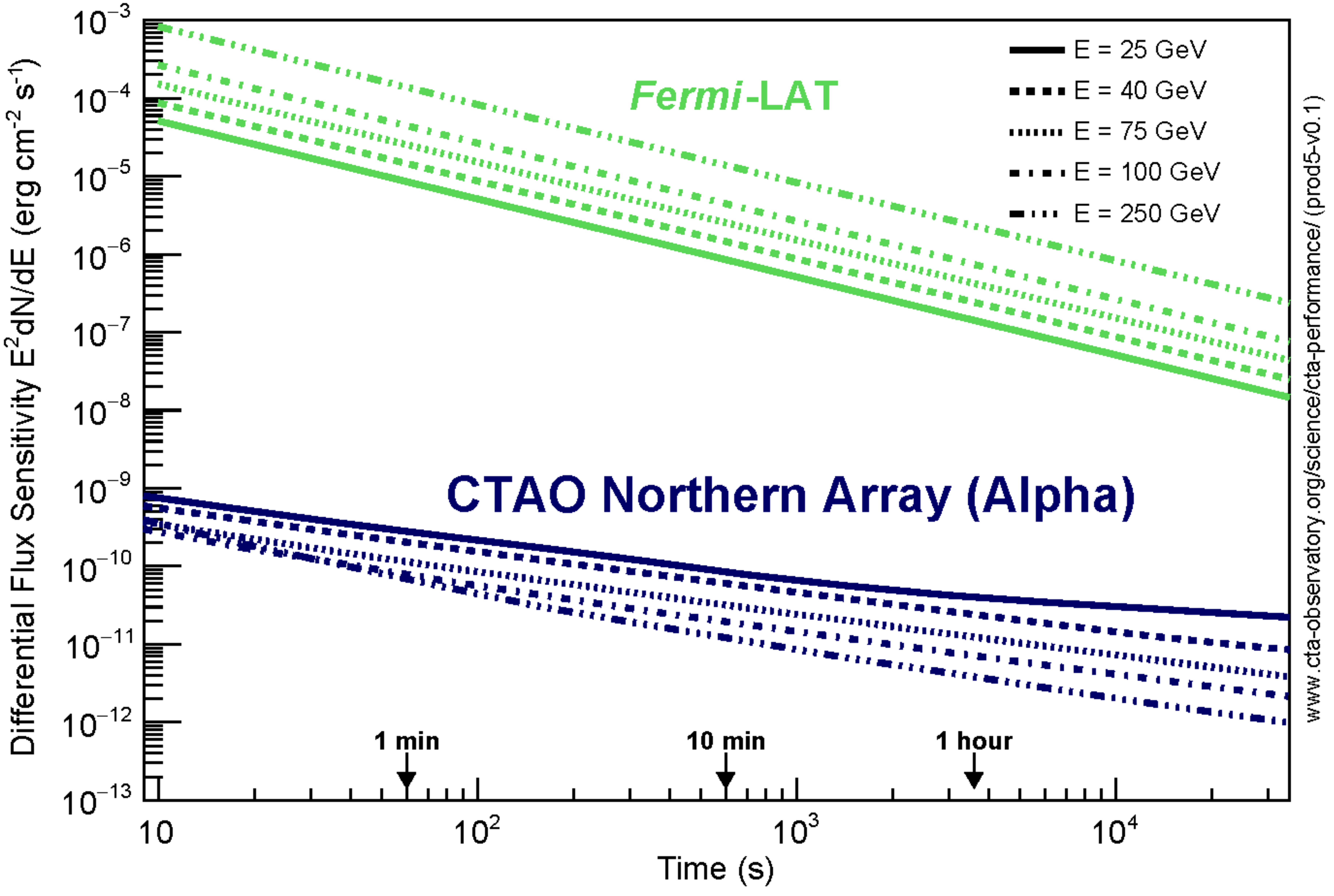

Fermi-LAT
CTAO Northern Array (Alpha)
E = 25 GeV
E = 40 GeV
E = 75 GeV
E = 100 GeV
E = 250 GeV
Differential Flux Sensitivity E²dN/dE (erg cm⁻² s⁻¹)
Time (s)
1 min
10 min
1 hour
www.cta-observatory.org/science/cta-performance/ (prod5-v0.1)

CTAO Northern Array
CTAO Southern Array
Angular Resolution (°)
Reconstructed Gamma-ray Energy E_R (TeV)
0.25
0.2
0.15
0.1
0.05
0
10^{-2}
10^{-1}
1
10
10^2
ASTRI
SWGO (inner)
MAGIC
HAWC
Fermi-LAT
VERITAS
https://www.cta-observatory.org/science/cta-performance (prod5, v0.1)

People involved in CTAO based in Bologna (in different forms/roles)

CTAO HQ. **R. Zanin** (CTAO project scientists)

Few people also at IRA (G. Migliori, extragal)

INAF-OAS/UniBo ~ 40 people

E. Bronzini (PhD, extragal)
G. Brunelli (PhD, gal)
A. Bulgarelli (software dev, ML)
M. Cappi (CTA+ scientific resp., extragal)
L. Castaldini (software dev, ML)
P. Da Vela (IGMF, extragal)
M. Dadina (extragal)
A. Di Piano (PhD, software dev, ML)
V. Fioretti (software dev, ML)
P. Grandi (extragal)

S. Marchesi (gal, extragal)
C. Nanci (IGMF, extragal)
N. Parmiggiani (software dev, ML)
G. Panebianco (software dev, ML)
V. Sguera (gal)
E. Torresi (extragal)
C. Vignali (extragal)